First Structural Investigation of a Super-Hydrated Zeolite

Yongjae Lee,[1] Thomas Vogt,[1] Joseph A. Hriljac,[2] John B. Parise,[3] and Gilberto Artioli[4]

[1]Physics Dept, Brookhaven National Laboratory, Upton, NY

[2]School of Chemical Sciences, The University of Birmingham, Birmingham, UK

[3]Geosciences Dept, State University of New York, Stony Brook, NY

[4]University Milan, Dipartimento Sci. Terra, Milan, Italy

Zeolites are naturally occurring aluminosilicates which crystallize in a variety of low-density framework structures built by corner-connected TO_4 (T = Al or Si)-tetrahedra.[1] These subunits connect to form a labyrinth of windows, pores and channels with molecular dimensions.[2] It is the restricted access through these windows to the interior that provides the reactant-, transition state and product-selectivity observed in zeolite catalysts. This selectivity makes these "nanoreactors" valuable selective heterogeneous catalysts and ion exchangers in a number of industrial and environmental applications. The built-in flexibility of the T-O-T angle between tetrahedral units allows these structures to contract and expand in response to thermodynamic variables such as temperature and pressure, thereby modifying their chemistry.

Our knowledge of pressure-induced phase transformations of zeolites is very limited compared to the vast number of temperature-dependent ones studied over the past several decades.[3-5] This is partly due to the experimental complexities as well as the analytical ambiguities arising from the porous nature of the materials, since this can lead to compositional changes upon interaction with various pressure-transmitting fluids where the molecular dimensions allow molecules to penetrate inside the zeolites.[6-8] Unusual effects such as negative thermal expansion and cation relocations in zeolite rho (~3.5 Å window to the interior) were found to be driven by temperature-induced chemical changes.[9] Therefore, applying external hydrostatic pressure was also likely to alter the chemical environment within the pores. Initially, we have found different phase transitions depending on the type of cations residing inside the pores of zeolite rho.[10] Various interaction schemes between cations and pressure-transmitting media have been proposed to drive the observed phase transitions in rho and other zeolites,[10-12] but no structural changes for these pressure-induced chemical changes have been reported to date.

Zeolite natrolite, which contains 2.5 Å pore openings, was studied using synchrotron x-ray powder diffraction as a function of pressure up to 5.0 GPa using a diamond-anvil cell (DAC) and a 200 mm-focused mono-

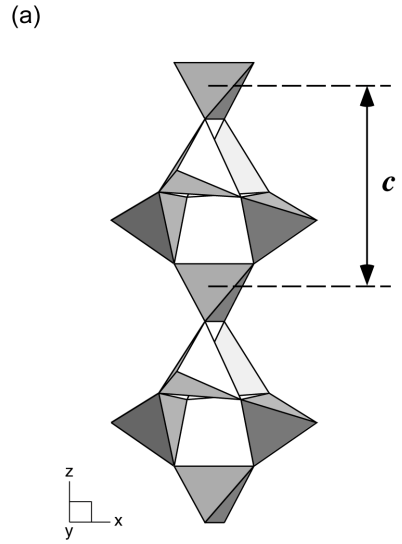

Figure 1. *(a) A polyhedral representation of the chain found in the NAT framework. The repeat distance of the T_5O_{10} building unit of five Si- (shaded) and Al- (unshaded) tetrahedra constitutes the* c*-axis length (***c***). (b) A simplified skeletal representation showing the channel along the* c*-axis. Vertices represent Al/Si tetrahedral atoms and oxygen atoms are omitted. The overall chain rotation angle, ψ, is an average value of ψ_a and ψ_b. An O2 oxygen is shown to visualize a T-O2-T angle.*

chromatic synchrotron X-ray beam (~0.7 Å). The natrolite framework is composed of T_5O_{10} tetrahedral building units that are connected along the *c*-axis forming the so-called natrolite chains (Figure 1a). The flexible linkages between and within the chains and their interactions with stuffed cations and waters give rise to various structural distortions depending on composition and temperature (Figure 1b). The high-pressure setup at beamline X7A at the National Synchrotron Light Source (NSLS) is shown in Figure 2. The powdered sample of the mineral natrolite (from Dutoitspan, South Africa, EPMA: $Na_{16}Al_{16}Si_{24}O_{80}{\cdot}16H_2O$)[13] was loaded into a 200 µm diameter sample chamber in a pre-indented Inconel gasket, along with a few small ruby chips as a pressure gauge. A mixture of 16:3:1 by volume of methanol:ethanol:water was used as a pressure medium (hydrostatic to above 10 GPa).[14] The pressure in the DAC was measured by detecting the shift in the R1 fluorescence line of the included ruby chips excited using an Ar laser. No evidence of nonhydrostatic conditions was detected during our experiments. Typically, the sample was equilibrated for about 15 min at each pressure, and the diffraction data were collected for 3 ~ 5 h (3 - 35° 2θ) using a position-sensitive gas-proportional detector (built by Graham Smith, BNL instrumentation division) gating on the Kr-escape peak. The pressure was then raised by 0.5 ~ 1.0 GPa increments up to 5 GPa. There was no evidence of stress-induced peak broadening or pressure-driven amorphization and after the experiment the recovered sample had its original white color, with its cell parameters similar to those at ambient conditions (within 3σ). Bulk moduli were calculated by fitting Murnaghan Equation of States to normalised volumes.

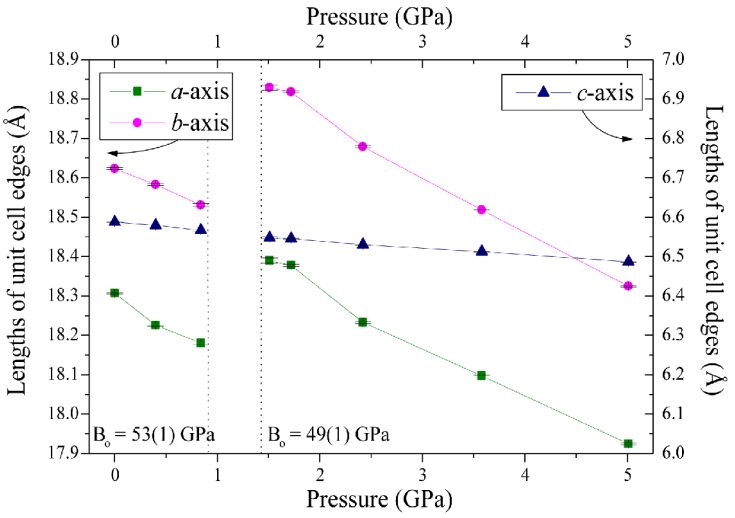

Figure 3. *Changes in the unit cell edge lengths (Å) of natrolite as a function of pressure. Estimated standard deviations are multiplied by three at each point. The structure model at ambient pressure is from the work of Baur et al.[20]*

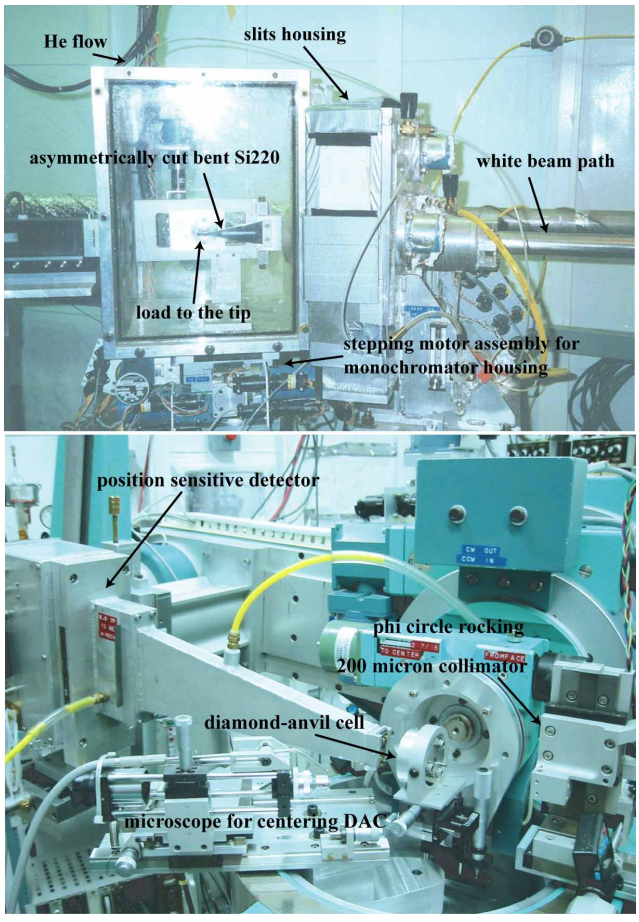

Figure 2. *High-pressure experimental setup as used at beamline X7A.*

The evolution of the unit cell parameters of natrolite is shown as a function of pressure in Figure 3. Between 0.8 and 1.5 GPa, the pressure-induced incorporation of water causes the expansion of the unit cell along the *a*- and *b*-axes whereas the *c*-axis shows an expected contraction. If one does not use an alcohol/water mixture as pressure-transmitting fluid but rather one where the molecules are too big to penetrate into the zeolites (e.g. silicone oil) this unit cell expansion is not observed. The anisotropic nature of the expansion suggests that the crystal structure responds to the pressure-induced adsorption of additional molecules by rotating the chains (Figure 1) along the *c*-axis. The resulting expansion of the channels in the (001) plane then leads to the observed volume increase. The mea-

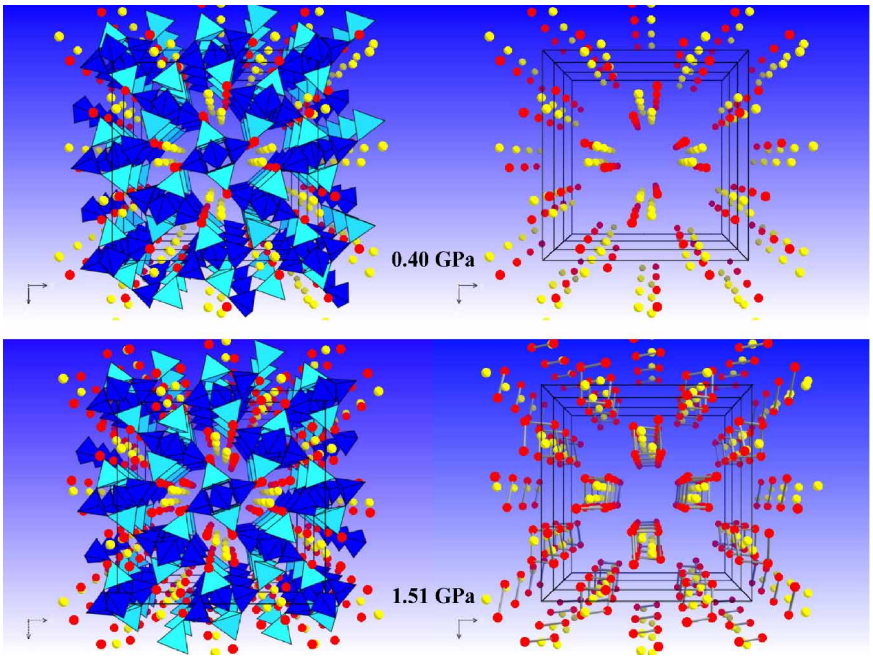

Figure 4. *Polyhedral representations of natrolite at (a) 0.40 GPa and (b) 1.51 GPa viewed along [001], the chain/channel axis. Each representation is repeated on the right without the framework component to emphasize the channel contents. Note the formation of the hydrogen-bonded water nanochain at 1.51 GPa. Red circles represent water molecules; yellow ones sodium cations. Blue (azure) tetrahedra illustrate an ordered distribution of Si (Al) atoms in the framework. Straight lines define the unit cell.*

sured bulk modulus of the large-volume natrolite (B_0 = 49(1) GPa) is slightly smaller than that of the normal natrolite (B_0 = 53(1) GPa), illustrating increased compressibility for this high-water-content phase.

We investigated the changes of the crystal structure accompanying the pressure-induced swelling by performing Rietveld refinements using the GSAS suite of programs.[15] The starting framework model at each pressure point was constructed from DLS-minimization,[16] which was later constrained during the refinement process. Difference Fourier maps were then generated, and sodium and oxygen atoms were used to model the extra-framework species (Na cations and water molecules, respectively). Refinement of the fractional site occupancies indicated that these atoms fully occupy the extra-framework sites, which were later fixed to unity. An overall isotropic displacement parameter was used for the framework atoms; another was used for the non-framework oxygens and cations. The two structural models for the phases before and after the volume expansion are shown in Figure 4. As the pressure increases up to 0.8 GPa, the water molecules shift away from the center of the $T_{10}O_{20}$ window, close to one of the bridging O(2) oxygens, resulting in an increase of the coordination number for the OW1 water from four (2 Na + 2 O) at 0.4 GPa to five (2 Na + 3 O) at 0.8 GPa. Considering only the extra-framework species, the water molecules and the sodium cations bond to form a chain along the *c*-axis (Figure 4a). After the volume expansion at 1.5 GPa, an additional fully occupied water site (OW2) is adsorbed

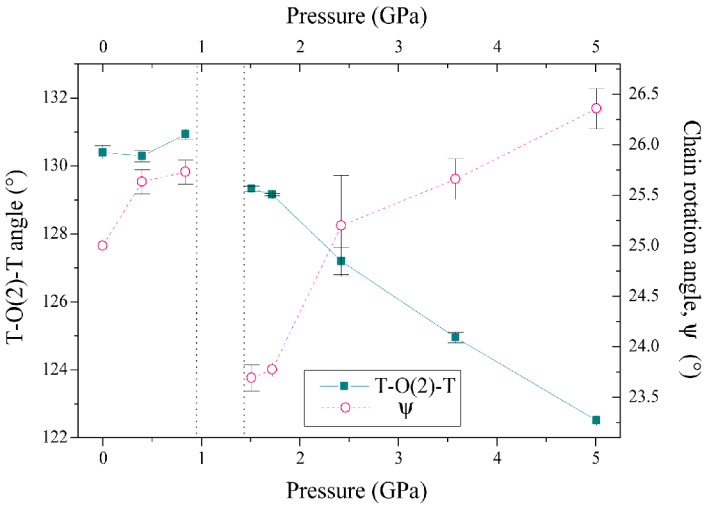

Figure 5. *Changes in T-O2-T bond angle and overall chain rotation angle of natrolite as a function of pressure.*

along the channel (Figure 4b) – hence the name superhydration resulting in a change of the water content of natrolite from 16 to 32 per unit cell. This new site has been proposed to be half-filled with water molecules in paranatrolite (24 H_2O per unit cell),[17] which results in to an anomalous increase of the water mobility in NMR and other spectroscopic measurements.[18,19] In fact, we observe a peak-splitting in the powder diffraction pattern at 1.25 GPa. Work is in progress to clarify this. The additional water molecule is coordinated by one sodium cation and six framework oxygens, forming a distorted capped trigonal prism. The OW1 water moves back to the center of the $T_{10}O_{20}$ window in a distorted tetrahedral environment. In contrast to the chain of sodium and water in the phase below 0.8 GPa, superhydration leads to a helical chain of hydrogen-bonded waters along the *c*-axis with O-O distances between 2.80(4) and 3.09(4) Å (Figure 4b). The position of the sodium cations does not show any appreciable changes during superhydration.

During the volume expansion and superhydration the changes in the framework geometry can be monitored by following the T-O-T bond angles within and between the chains (Figure 1). The T-O-T angles within the chain do not reveal any systematic changes whereas the bridging T-O2-T angle between the chains shows small changes before, and a continuous contraction after superhydration (Figure 5). Before superhydration the overall chain rotation angle, ψ (Figure 1b) increases initially up to 25.7° at 0.8 GPa, then drops to 23.7° during superhydration, and increases back up at higher pressures (Figure 5). This indicates that superhydration is tied to the relaxation of the overall distortion of the framework by expanding the pore space in the plane perpendicular to the channel.

Diffraction data on the recovered sample indicate the reversibility of the system. Pressure-induced hydration (or other chemical changes) in other members of fibrous zeolites are currently being investigated. The changes observed in these materials hint that pressure-induced expansion is a promising way of extending the ion exchange and sorption capacities, and possibly selectivities, of open framework structures. This could lead to potential applications involving "trap-door" ion exchange. By exchanging cations under pressure the larger opening permits larger cations (e.g ^{90}Sr) to penetrate into the pores. On subsequent pressure release they will remain trapped inside the material resulting in very low leaching rates. We hope that by modifying the framework composition we will be able to stabilize a superhydrated zeolite at ambient condition. This could be used to store, for example, tritium-exchanged water. Superhydration is also considered a possible mechanism for the storage and transport of water into the Earth's upper mantle, since the conditions found for superhydration to occur resemble part of the cold oceanic lithosphere during subduction processes.

Acknowledgment

This work was supported by an LDRD from BNL (Pressure in Nanopores). J. Parise is grateful for support from grants ACS-PRF and NSF (DMR-0095633). Research carried out in part at the NSLS at BNL is supported by the U.S. DoE, Division of Materials Sciences and Division of Chemical Sciences under Contract No. DE-AC02-98CH10886. We acknowledge the Geophysical Lab of the Carnegie Institute for allowing us the use of the ruby laser system of beamline X17C.

References

[1] Breck, D.W. *Zeolite Molecular Sieves*; Krieger: Malabar, FL, 1984.
[2] Baerlocher, C.; Meier, W.M.; Olson, D.H. *Atlas of Zeolite Framework Types*; 4th ed.; Elsevier: Amsterdam, 2001.
[3] Corbin, D.R.; Abrams, L.; Jones, G.A.; Eddy, M.M.; Harrison, W.T.A.; Stucky, G.D.; Cox, D.E. *J. Am. Chem. Soc.* **1990**, *112*, 4821.
[4] Baur, W.H.; Joswig, W. *N. Jb. Miner. Mh.* **1996**, 171.
[5] Artioli, G. *In situ structural and kinetic powder diffraction studies of aluminosilicates*; Wright, K. and Catlow, R., Ed.; Kluwer: Dordrecht, 1999; Vol. NATO Sciences Series C, pp 177.
[6] Hazen, R.M. *Science* **1983**, *219*, 1065.
[7] Knorr, K.; Braunbarth, C.M.; van de Goor, G.; Behrens, P.; Griewatsch, C.; Depmeier, W. *Solid State Commun.* **2000**, *113*, 503.
[8] Rutter, M.D.; Uchida, T.; Secco, R.A.; Huang, Y.; Wang, Y. *J. Phys. Chem. Solids* **2001**, *62*, 599.
[9] Lee, Y.; Reisner, B. A.; Hanson, J.C.; Jones, G.A.; Parise, J.B.; Corbin, D.R.; Toby, B.H.; Freitag, A.; Larese, J.Z.; Kahlenberg, V. *J. Phys. Chem.* **2001**, *B105*, 7188.
[10] Lee, Y.; Hriljac, J.A.; Vogt, T.; Parise, J.B.; Edmondson, M.J.; Anderson, P.A.; Corbin, D.R.; Nagai, T. *J. Am. Chem. Soc.* **2001**, *123*, 8418.
[11] Hazen, R.M.; Finger, L.W. *J. Appl. Phys.* **1984**, *56*, 1838.
[12] Belitsky, I.A.; Fursenko, B.A.; Gubada, S.P.; Kholdeev, O.V.; Seryotkin, Y. V. *Phys. Chem. Minerals* **1992**, *18*, 497.
[13] Artioli, G.; Smith, J. V.; Kvick, A. *Acta Cryst.* **1984**, *C40*, 1658.
[14] Hazen, R.M.; Finger, L.W. *Comparative Crystal Chemistry*; John Wiley & Sons: New York, 1982.
[15] Larson, A.C.; VonDreele, R.B. "GSAS; General Structure Analysis System," Los Alamos National Laboratory, New Mexico, 1986.
[16] Meier, W.H.; Villiger, H. *Z. Kristallogr.* **1969**, *129*, 411.
[17] Baur, W.H. *Crystal Research and Technology* **1991**, *26*, 169.
[18] Moroz, N.K.; Kholopov, E.V.; Belitsky, I. A.; Fursenko, B. A. *Microporous Mesoporous Mater.* **2001**, *42*, 113.
[19] Gabuda, S.P.; Kozlova, S.G. *J. Struc. Chem.* **1997**, *38*, 562.
[20] Baur, W.H.; Kassner, D.; Kim, C.-H.; Sieber, N.H. *Eur. J. Mineral.* **1990**, *2*, 761.